UNIVERSITY OF BIRMINGHAM

A New Reservoir Of Lithium Production In A Metal-Poor Universe

Sam Ratcliff

Student ID: 1425093

Project Supervisors: Dr. Dorottya Szécsi, Prof. Ilya Mandel
Project Partner: Nick Bennett
Word Count: 7591

March 23, 2018

School of Physics and Astronomy
University of Birmingham
Birmingham, B15 2TT

Contents

1 Abstract **2**

2 Introduction **2**
2.1 Motivation . . . 2
2.2 Methods . . . 2

3 Theory **4**
3.1 Lithium in the Universe . . . 4
3.2 Stellar Evolution . . . 5
3.2.1 Main Sequence . . . 5
3.2.2 Post-Main Sequence . . . 5
3.2.3 Kippenhahn Diagrams . . . 6
3.3 Globular Clusters . . . 7
3.4 Multiple Populations and Anti-Correlations . . . 7
3.5 Initial Mass Function . . . 8

4 Results **9**
4.1 Anti-correlations . . . 9
4.2 Surface Lithium . . . 10
4.3 Lithium Production Method . . . 11
4.4 Changing Mass . . . 12
4.5 Changing Rotational Velocity . . . 14
4.6 Lithium Pollution . . . 15

5 Conclusion **16**

A Appendix **20**
A.1 Kippenhahn Diagrams . . . 20
A.2 High Rotation Model . . . 20
A.3 Radius Plot . . . 21

1 Abstract

Lithium is a light element synthesised in the first few minutes of the Universe but is destroyed by the high temperatures required for nuclear fusion in a star's core. Therefore it is unclear why high lithium abundance is observed in some second generation stars in globular clusters which are thought to have formed from the nuclear processed materials ejected by massive stars in the previous generation. We have run models for several low metallicity, massive stars which could pollute next generations of stars with nuclear processed materials. We find that, initially, the lithium in their cores is destroyed, and rotational mixing within the stars carries this depleted material out to the surface causing the surface lithium abundance to decreases over time. However, when the star has started core helium burning, models show a jump in the surface lithium abundance. This suggests that lithium production is taking place in massive stars which could explain globular cluster observations. Lithium is produced by the pp chain in the hydrogen burning shell during these stars post-main sequence, and is mixed out of the nuclear burning region to the surface by a deep convective envelope, without which the lithium would be destroyed. These massive star then pollute the intra-cluster medium with lithium enriched material by stellar winds or binary stripping. This nuclear processed material exhibits both the high lithium abundance and the anti-correlation effects observed in some globular clusters. Therefore, massive stars such as the ones modelled here could be candidates for explaining these abundance anomalies. We estimate up to an order of magnitude of 10^3 solar mass stars in a cluster of 10^6 stars could be formed from lithium-enriched material ejected by these massive stars.

2 Introduction

2.1 Motivation

The aim of this project is to create stellar models of massive stars to show how the abundances of lithium vary as they age and to try and explain the observational results from globular clusters. Lithium is destroyed by the high temperatures in a star's core and as this lithium-depeleted material is mixed throughout the star, we would expect a very low lithium abundance in, for example, post main-sequence stars. For the most part, this is what is observed. For example, in Pilachowski et al. (2000), a survey of 261 post-main sequence giants in several different globular clusters was carried out and all of the stars were found to be very lithium-poor— from this an upper limit of the lithium abundance was set at A(Li) < 1. However, there have also been some observations of high lithium abundance anomalies in turn off stars and intermediate mass, AGB (asymptotic giant branch) stars (Monaco et al., 2012; Carney et al., 1998) with values as high as A(Li) $= 2.87$. This suggests another form of lithium production or enrichment exists that is unaccounted for. Pollution or enrichment by a previous generation of stars has previously been suggested in order to explain abundance anomalies and anti-correlations of elements in globular clusters (Prantzos et al., 2007; Pasquini et al., 2005). Pollution of the intra-cluster medium (ICM) by enriched gas from AGB stars was proposed in Pasquini et al. (2005), however it could not explain all the observed features at once which suggests there is another, unaccounted for process occurring. In particular, this mechanism of enrichment could not explain the anomalous high lithium abundance. This paper goes on to suggest that alternative mechanisms should be explored in order to fully explain these observations.

2.2 Methods

We have used the Binary Evolution Code (BEC), and in particular the BEC interface, to create models of massive, low metallicity, single stars in the initial mass range $45M_\odot$ to $100M_\odot$. These stars are being modelled as a previous generation of massive stars that could pollute a cluster with enriched materials

and produce the abundance anomalies observed today. BEC is a stellar evolution code that models the lifetime of both single stars and binary stars; although only single stars have been modelled in this project. BEC assumes spherical symmetry and creates one dimensional models of stars according to some input parameters as shown below:

- The mass of the star in solar masses, M.
- The metallicity of the star, Z.
- The initial rotational velocity of the star, v.
- The reference point for the metallicity: i.e. Z is given as a fraction of the metallicity of the Large Magellanic Cloud (lmc), the Small Magellanic Cloud (smc) or the Milky Way (mw).

From these initial parameters, BEC then evolves this star using hydrodynamics and by considering nuclear processes such as the pp chain, the CNO cycle and other burning reactions for heavier elements. BEC outputs several parameters including surface temperature, density and luminosity. However, the main output parameters to be considered initially are the relative abundances of the different elements throughout the star— primarily lithium.

When we consider the abundances of different elements within stars, we do not use their absolute value but their relative abundance compared to hydrogen. For example, when considering the abundance of iron, we would measure this as [Fe/H] as shown below in equation (1).

$$[Fe/H] = \log_{10}\left(\frac{Fe}{H}\right) - \log_{10}\left(\frac{Fe}{H}\right)_{\odot} \tag{1}$$

Where Fe and H are the number of iron and hydrogen atoms respectively per unit volume in the star. The second term is the solar values for these quantities and so a star with [Fe/H]=0 has the same iron to hydrogen ratio as the Sun. Often abundances of elements are given in reference to the iron content of a star as shown below in equation (2)

$$\begin{aligned} [Na/Fe] &= \log_{10}\left(\frac{Na}{Fe}\right) - \log_{10}\left(\frac{Na}{Fe}\right)_{\odot} \\ [Na/Fe] &= \left[\log_{10}\left(\frac{Na}{H}\right) - \log_{10}\left(\frac{Na}{H}\right)_{\odot}\right] - \left[\log_{10}\left(\frac{Fe}{H}\right) - \log_{10}\left(\frac{Fe}{H}\right)_{\odot}\right] \end{aligned} \tag{2}$$

When measuring the abundances of lithium in this project we use units of A(Li) and by substituting in values for the lithium and hydrogen abundances in the sun we get equation (3).

$$\begin{aligned} A(Li) \equiv [Li/H] &= \log_{10}\left(\frac{Li}{H}\right) - \log_{10}\left(\frac{Li}{H}\right)_{\odot} \\ &= \log_{10}\left(\frac{Li}{H}\right) + 12 \end{aligned} \tag{3}$$

3 Theory

3.1 Lithium in the Universe

In the past, it was thought that the first stars formed were comprised entirely from hydrogen, with heavier elements being generated by fusion in the star. These first stars would then pollute future generations of stars causing the abundance of elements that we see in the universe today. While this is true for some elements, it is now thought that this is not the case for the light elements, deuterium, helium 3, helium 4 and lithium, with these elements instead being produced in the early universe in Big Bang nucleosynthesis. This model set the expected lithium abundance for when the formation of stars began.

After the Big Bang, the Universe expands and cools rapidly. While initially the Universe is too hot for nuclei to form, it eventually cools to a temperature low enough for this to take place. This is the process called Big Bang nucleosynthesis by which the light elements were made in the first few minutes of the universe (normally approximately defined as 10 seconds to 20 minutes after the Big Bang) during the radiation dominated era when temperatures were $\lesssim$ 1MeV (Fields et al., 2013). This corresponds to an average nuclear binding energy, so if a typical photon has an energy >1MeV, then nuclei will not form (Liddle , 2013). During the period of nucleosynthesis, the light elements are formed, until the density and temperature of the Universe drop too low for fusion to continue to take place. Tritium (^{3}H) and beryllium-7 are also produced but these are unstable so quickly decay to ^{3}He and ^{7}Li respectively. Some important reactions in the formation of light elements are shown below (Liddle , 2013):

$$p + n \rightarrow D \tag{4}$$

$$D + p \rightarrow {}^3\mathrm{He} \tag{5}$$

$$D + D \rightarrow {}^4\mathrm{He} \tag{6}$$

From here, heavy nuclei are formed by the processes of nuclear fusion within the star (or during supernova explosions). The two processes by which nuclear fusion of hydrogen into helium occur in a star are the pp (proton-proton) chain and the CNO (carbon-nitrogen-oxygen) cycle— the former dominating in the core of stars around the mass of the sun and less, and the latter dominating in the core of more massive stars such as the ones being considered in this project. An example of one of the branches of the pp chain is shown below. The pp chain is important when considering lithium, as lithium is produced as a by-product of one of the branches (as shown in equation (11)). However, this lithium is then destroyed by the next reaction in the chain as shown in equation (12). A possible cause for higher lithium abundances in stars is that they have been enriched by previous generations of stars in their formation; causing them to have higher abundances of heavier elements (Pasquini et al., 2005), (Monaco et al., 2012), but this requires some form of lithium production to take place.

$${}^1_1\mathrm{p} + {}^1_1\mathrm{p} \rightarrow {}^2_1\mathrm{H} + \mathrm{e}^+ + \nu_e \tag{7}$$

$${}^2_1\mathrm{H} + {}^1_1\mathrm{p} \rightarrow {}^3_2\mathrm{He} + \gamma \tag{8}$$

$${}^3_2\mathrm{He} + {}^3_2\mathrm{He} \rightarrow {}^4_2\mathrm{He} + {}^1_1\mathrm{p} + {}^1_1\mathrm{p} \tag{9}$$

$${}^3_2\mathrm{He} + {}^4_2\mathrm{He} \rightarrow {}^7_4\mathrm{Be} + \gamma \tag{10}$$

$${}^7_4\mathrm{Be} + e^- \rightarrow {}^7_3\mathrm{Li} + \nu_e \tag{11}$$

$$^{7}_{3}\mathrm{Li} + ^{1}_{1}\mathrm{p} \rightarrow ^{4}_{2}\mathrm{He} + ^{4}_{2}\mathrm{He} \tag{12}$$

3.2 Stellar Evolution

3.2.1 Main Sequence

Once the main sequence lifetime of a star starts, hydrogen fusion in the star's core acts as its energy source and stops the star from gravitational collapse, leaving the star in a stable state where it spends most of its lifetime. The 2 nuclear reactions of hydrogen burning take place in the star's core, the pp (proton-proton) chain and the CNO (carbon-nitrogen-oxygen) cycle, with the CNO cycle contributing a significant fraction of the star's energy for stars of above $1M_{\odot}$ and dominating at masses above about $1.5M_{\odot}$. This is because the CNO cycle becomes more efficient as temperatures are increased and so it dominates for more massive, high temperature stars.

Massive stars radiate away energy at a greater rate than low mass stars which means they have a shorter lifetime. The main sequence lifetime of a star roughly follows the power law $\tau_{MS} \propto M^{\alpha}$ where M is the mass of the star and $\alpha \approx -2.5$.

3.2.2 Post-Main Sequence

During their post-main sequence lifetime, massive stars diverge most noticeable from other stars in their evolutionary path; the following stages of evolution apply to high mass stars. When the hydrogen in the star's core is exhausted, the core starts to contract as there is no longer an outward pressure provided by hydrogen fusion. This contraction increases the core temperature and pressure until it is sufficient to start helium fusion in the star's core. The outer envelope of the star expands and cools leaving the star in the red supergiant phase. Stars above about $40M_{\odot}$ (at solar metallicity) however, have very high stellar winds due to their high luminosity and hence tend to lose mass from their outer envelope and never actually become red supergiants. Stars in this mass range therefore retain their high temperatures in their post-main sequence lifetimes. This can occur due to partial ionisation of hydrogen in the outer layers which drives an oscillation in such massive star, often leading to mass being ejected (Yoon et al., 2013; Li et al., 1994). However, this is not the case for the low metallicity stars being modelled in this project.

Helium fusion starts in the core of the star which is surrounded by a hydrogen shell, but this helium burning lifetime only lasts as long as 10% of the main sequence lifetime. Once the helium core is exhausted, the core starts to contract until temperatures are high enough for carbon fusion to begin. Similarly, the star will then be composed of a carbon core surrounded by first a helium, then a hydrogen shell. Each element that is fused in the core will have a progressively shorter and shorter lifetime as the elements become heavier (just as the helium core was exhausted quicker than the hydrogen core). This continues with other elements such as oxygen and silicon until the star has an iron core, with shells of other elements in layers all the way out to a hydrogen shell. Unlike other elements, however, nuclear fusion of iron does not produce a net positive output of energy and instead uses up energy, as iron is the most stable nuclei. This means the core starts to contract. This has the runaway effect of increasing the rate of fusion, which cools the core and causes more contraction. If the mass of the core is above a threshold mass of around $1.4M_{\odot}$ (the Chandrasekhar limit), the electron degeneracy pressure is not sufficient to balance the gravitational force of the star's collapse and so a core collapse supernova takes place (Janka., 2006). This is when material expelled outwards by the core collapse meets material from the star collapsing towards the core, causing a shock wave. Supernovae not only

provide the conditions required for nuclear fusion of heavier elements, but also expel them with a high velocity which disperses them throughout the Universe.

3.2.3 Kippenhahn Diagrams

A Kippenhahn diagram is a 2 dimensional plot of a star which shows how its internal structure evolves throughout time. For example, a Kippenhahn diagram often shows distinct regions (indicated by different colours) such as the convective and overshoot mixing zones of a star. Time is plotted on the x axis and the mass coordinates of the star (in solar masses) on the y axis. They often have a contour scale to show where in the star nuclear burning is taking place. From this, we can observe how the size and location of convective and nuclear burning regions evolve throughout a star's lifetime and identify specific events in a star's lifetime such as the exhaustion of the hydrogen core. Kippenhahn diagrams are built up by plotting mass coordinates that fit certain criteria (i.e. the Schwarzschild criterion for convection) for each time step to build up a visual representation of the evolution of structure within a star.

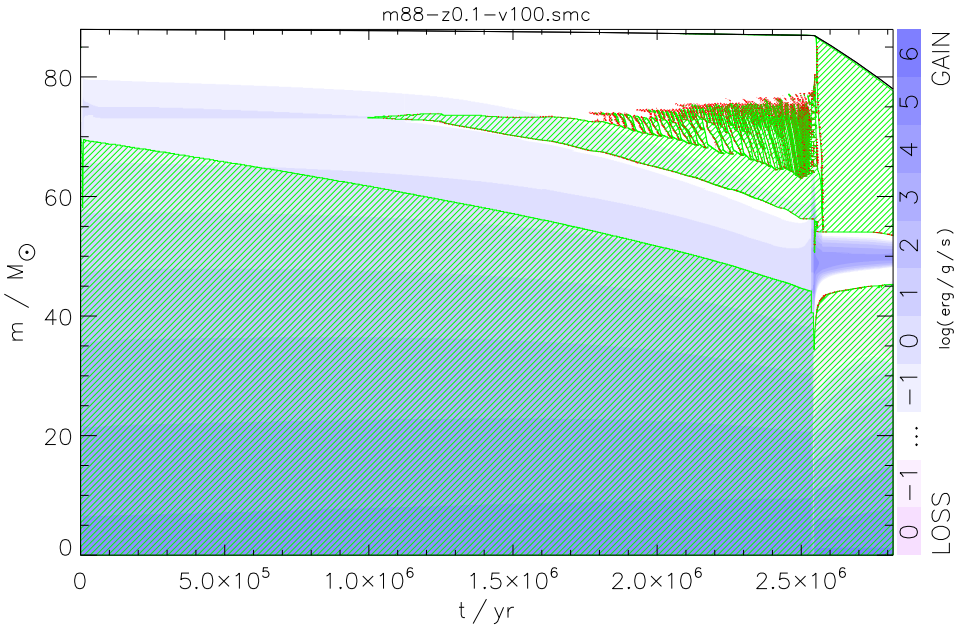

Figure 1: Kippenhahn diagram for $88M_{\odot}$ model.

Figure 1 shows a Kippenhahn diagram for an $88M_{\odot}$ model and highlights the internal structure of these massive stars being modelled in this project. The green hatched areas on the plot indicate convective regions within the star, the red shading indicates semi-convective regions and the contour energy scale at the side of the plot indicates regions of energy production (nuclear burning regions). The solid black line shows the mass at the surface of the star and hence the change in total mass of the star throughout its lifetime. The main sequence part of the star's lifetime comprised most of the star's lifetime and the hydrogen burning core can be seen on the plot between 0 and 2.55Myr.

During the start of the main sequence lifetime of these massive stars, they have a convective core surrounded by a non-convective region at the surface. Later on in its main sequence lifetime, this

convective region in the core is smaller but still surrounded by a non-convective region. These stars also develop another convective region further away from the core but the surface remains non-convective. When the hydrogen in the core is exhausted, the core contracts until helium core ignition and the star begins its helium core burning lifetime. At this post-main sequence stage in the lifetime of these massive stars, there is a notable shift in the star's structure, as illustrated by the Kippenhahn diagram at around 2.55Myr. Not only is there nuclear fusion occurring in the core, but we also observe a shell of nuclear fusion further out in the star— this corresponds to hydrogen shell burning. Another change in the internal structure is that the outer convective region now reaches all the way from this hydrogen burning shell to the surface of the star. It can also be seen that during the post-main sequence phase, the total mass of the star decreases at a much greater rate than previously which indicates this is the part of a massive star's lifetime where the mass loss rate is the highest.

3.3 Globular Clusters

A globular cluster is a gravitationally bound collection of up to a few million stars, typically found in galactic halos. Globular clusters are dense regions of old, metal poor stars (Population-II) and are thought to have formed relatively soon after the Big Bang. Globular clusters tend to have very little interstellar gas as it has largely been used up in star formation long ago. Globular clusters have such long lifetimes because they are so strongly gravitationally bound and this long lifetime means that they consist mainly of fairly cool, fairly low mass stars. This is because the lifetime of a star is shorter for massive, hotter stars so these stars are not observed in globular clusters as their lifetimes are much shorter than that of the cluster.

It is also useful to look at the chemical compositions of globular clusters as they would have formed from the proto-cluster gas fairly soon after the Big Bang and so can be used to test models of Big Bang nucleosynthesis and nuclear burning to see if they predict the observed abundances. They can also be observed to see how more massive stars that evolve more quickly can pollute the rest of the cluster with heavier elements (Prantzos et al., 2007; Harris et al., 2006; Gratton et al., 2004).

3.4 Multiple Populations and Anti-Correlations

Globular clusters were once thought to be simple stellar populations all made from one generation of stars, formed at the same time. These stars would have a range of masses according to the initial mass function and would have essentially the same initial abundances of elements. However, it is now thought that globular clusters are actually made up of multiple populations of stars (ranging from 2 to up to 6 generations, Bellini et al., 2010) formed at different times. This is due to an observed range of different abundances of light elements in stars that suggest a pollution of elements fused in the high temperatures of a star's core in a previous population. Another piece of evidence for this is by looking at the colour-magnitude diagram for certain globular cluster where some of the features seen (such as the horizontal branch) cannot be explained by a single stellar population alone. The first observational evidence of multiple populations was published in Bedin et al. (2004), where the data showed a splitting of the main sequence.

The idea of multiple generations is needed to explain these chemical inhomogeneities, as this allows effects such as pollution from ejection from massive or intermediate mass stars to pollute the cluster, from which the next generation of stars is formed (Henault-Brunet et al., 2015). One way this material is ejected is by stars on the asymptotic giant branch (AGB) of the Hertzsprung-Russell diagram, which are intermediate mass post main sequence stars that have expanded to many times their initial radii. Because of these large radii, material can be ejected by stellar winds on these stars at relatively low

velocities due to the lower escape velocity which is a result of the star's size. This lower velocity means that material ejected by AGB stars does not have the escape velocity to leave the cluster so will remain in the ICM and pollute the next generation. There is also another way AGB stars can be responsible for the pollution that does not require too much mass to be lost: early disc accretion. This is when AGB stars eject enriched material in the central regions of clusters, and stars that pass through this central region get enriched by accreting the material (Henault-Brunet et al., 2015).

Another piece of evidence supporting the idea of multiple populations is the anti-correlation of light elements occurring in low mass main sequence stars. These anti correlations are observed between elements such as carbon and nitrogen (arising from the CNO cycle) and for other elements such as aluminium and magnesium (arising from the high temperature Mg-Al cycle). Anti-correlation of elements gives strong evidence for them having been produced in sufficiently high temperatures in hydrogen burning reactions. Thus observations of anti-correlations of certain elements in low mass stars, where the temperatures are not high enough for the corresponding nuclear reaction to have taken place, indicate that these elements must have been formed in other high mass stars which have polluted the low mass stars (Denissenkov et al., 2015).

3.5 Initial Mass Function

Stellar populations are made up of a wide range of stars of different masses which are weighted by a mass function. The initial mass function (IMF) gives the distribution of the number of stars in each mass range originally in a star-forming region. This function models the fact that solar mass stars like the Sun, for example, are a lot more abundant than $50M_{\odot}$ stars. The initial mass function is important in many areas of astrophysics and cosmology as the amount of massive stars in a galaxy determines the galaxy's chemical make-up and its evolution (Chabrier , 2003). The IMF was first formulated in Salpeter (1955) and is shown in equation (13). $\zeta(m)$ is defined as the number of stars in a mass interval, or $\zeta(m) = \frac{dn}{dm}$ where n is the stellar number density (number of stars per unit volume).

$$\begin{aligned} \zeta(m) &\propto m^{-\alpha} \\ \alpha &\sim 2.3 \end{aligned} \tag{13}$$

The IMF is essentially a probability distribution function of the mass of a star when it starts its lifetime and so $\int_0^{\infty} \zeta(m)dm = 1$. For example, to find out the number of stars we would expect to find in the mass range $50M_{\odot}$-$60M_{\odot}$ in a sample of N_{total} stars, we would evaluate the expression shown in equation (14).

$$N = N_{total} \cdot \int_{50M_{\odot}}^{60M_{\odot}} m^{-2.3} dm \tag{14}$$

4 Results

We have used the Binary Evolution Code (BEC) interface to create models of massive, low metallicity, single stars that could pollute a cluster with enriched materials. The models created are shown in Table 1. These stars all have an initial metallicity of $Z = 0.1Z_{smc} \sim 0.02Z_{\odot}$ where Z_{smc} is the metallicity of the Small Magellanic Cloud and $Z_{\odot}$ is the metallicity of the sun. These are very low metallicity models that would be in one of the first generations of stars so are candidates for polluting future generations and potentially causing the observed abundance anomalies (Szécsi et al., 2015).

Table 1: Table showing the models created and their input parameters. All these models have a metallicity of $Z = 0.1Z_{smc} \sim 0.02Z_{\odot}$.

Initial Mass [$M_{\odot}$]	Initial Rotational Velocity [km/s]
45	100
66	100
74	100
77	50
	75
	100
	125
82	100
88	100
100	100

These models have been run from the start of the star's lifetime, throughout the main sequence lifetime and past core hydrogen exhaustion, until approximately the point of core helium exhaustion (post-main sequence). From here, these stars start to fuse heavier elements in their cores. However, for these high mass stars being considered in this project, this part of the star's lifetime happens over such a short amount of time that this can be neglected. Therefore we can fairly say, for example, that the amount of lithium produced during the star's core hydrogen and core helium burning lifetimes corresponds to essentially the total amount produced in its lifetime.

4.1 Anti-correlations

Initially, the abundances of various elements were plotted in order to observe correlations and anti-correlations of elements that are produced in massive stars, to show that the polluted material from these stars would also show these relations as in observations. An example of anti-correlations produced by these models is shown in Figure 2 which shows an anti-correlation between magnesium and aluminium. This indicates that the high temperature Mg-Al chain is taking place in these massive stars (Ventura et al., 2011). These massive stars could then go on to pollute low mass stars with those nuclear burning products which are shown in observations today. Figure 3 shows the abundances of sodium, magnesium and aluminium plotted against the abundance of oxygen (all relative to iron). These elements were chosen as they have all been observed to have correlation/anti-correlation effects with oxygen which may arise from nuclear fusion reactions. These plots are for 3 models created ($45M_{\odot}$, $77M_{\odot}$ and $100M_{\odot}$), although other models also reproduce these relations. This shows that these models are capable of reproducing correlations/anti-correlations of elements observed in many studies such as Denissenkov et al. (1997).

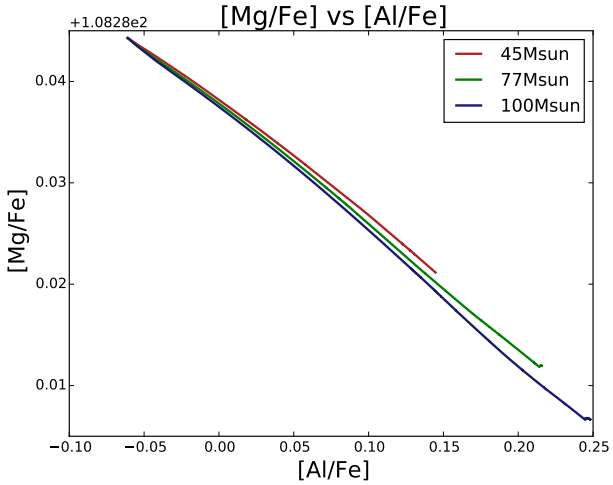

Figure 2: Plot of magnesium abundance against aluminium for $45M_{\odot}$ $77M_{\odot}$ and $100M_{\odot}$ models, showing the anti-correlation that indicate the presence of a high temperature fusion reaction, the Mg-Al chain.

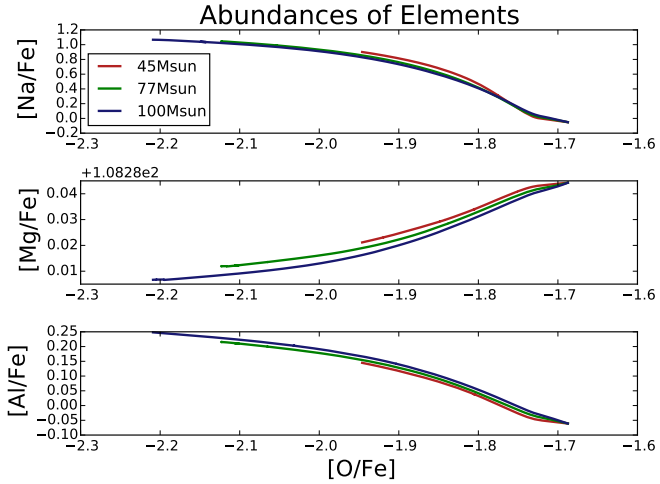

Figure 3: Plot of element abundances against oxygen for $45M_{\odot}$ $77M_{\odot}$ and $100M_{\odot}$ stars, showing the correlation/anti-correlation effects that indicate the presence of high temperature fusion reactions, such as the Mg-Al chain and the Ne-Na chain.

4.2 Surface Lithium

A graph of the surface lithium through the star's lifetime was also plotted for the $77M_{\odot}$ model in Figure 4. This plot shows the initial depletion in surface lithium throughout time as it is destroyed in the core by the high temperatures and this depleted material is transported out to the surface layers by rotational mixing. The initial abundance of lithium at $t = 0$ is essentially that produced by Big Bang nucleosythesis as this is at a very low metallicity where very little nuclear processing of the ICM gas has taken place. An observational value of high lithium abundance of an AGB star in a globular cluster from Carney et al. (1998) is also plotted for comparison. These models show a sharp jump in surface lithium later in their lifetimes which, in the case of this model, reaches up to a value comparable

to that from observations. From here, the surface lithium fraction remain roughly at the same level. This jump shows a previously unaccounted for method of lithium production within massive stars and could help to explain the lithium abundance anomalies observed in globular clusters. The mechanisms responsible for this jump in lithium are described in section 4.3.

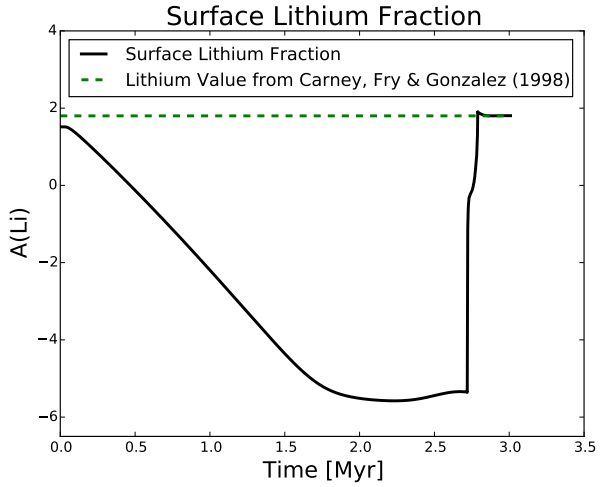

Figure 4: Plot of surface lithium for $77M_{\odot}$ star with dotted line showing observational value from Carney et al. (1998).

4.3 Lithium Production Method

To understand this method of lithium production, the internal structure of massive stars must be considered. Figure 5 is a Kippenhahn diagram for the $77M_{\odot}$, v=75km/s model, and Figure 6 is the same plot but zoomed in as the star goes from core hydrogen to core helium burning, where the lithium production takes place.

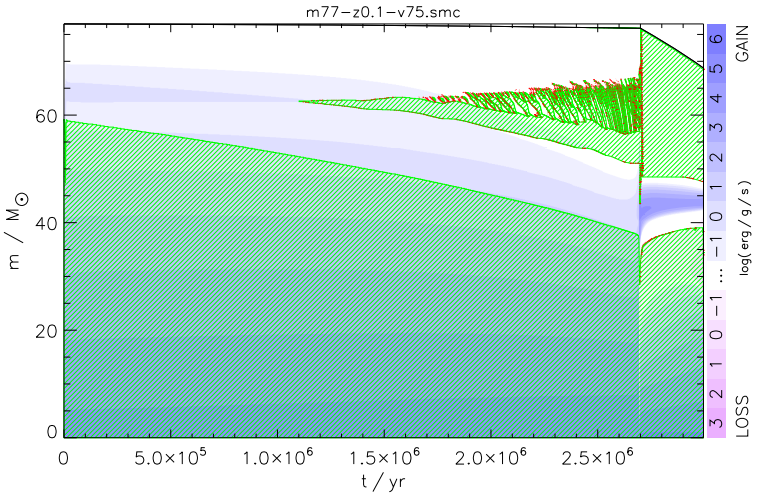

Figure 5: Kippenhahn diagram for $77M_{\odot}$, v=75km/s model.

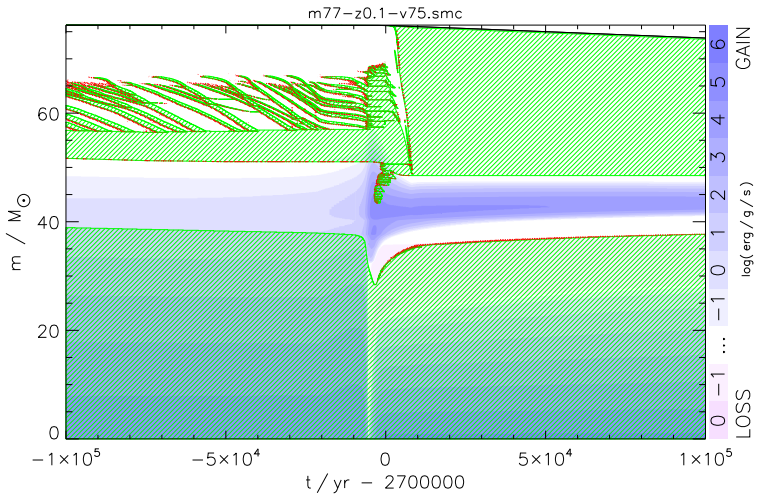

Figure 6: Kippenhahn diagram for $77M_{\odot}$, v=75km/s model zoomed in at around the onset of core helium fusion.

The time when the lithium production occurs in these massive stars is when they end their main sequence lifetimes and start nuclear fusion of helium in their cores. This causes a change in the stars internal structure. As well as helium core burning, the energy scale on the diagram shows that hydrogen shell burning is also taking place. Previously in these massive stars, the CNO cycle was the dominant nuclear process responsible for hydrogen fusion due to the high temperatures in the cores of these massive star. When this hydrogen shell fusion takes place, however, this is outside of the core of the star where the temperatures are less and so, in these regions, the pp chain is the dominant process. Looking again at the pp chain, we see that lithium is produced in one of the branches as shown in equation (11) before it is subsequently destroyed by proton capture in the next reaction in the chain, in equation (12). However, when there is hydrogen shell burning taking place, there is a deep convective envelope that reaches all the way down into this nuclear burning region. This can be seen more clearly in Figure 6, where we see an overlap in the green convective region and the blue nuclear burning region around the time of helium core ignition. This means that the lithium produced in this shell can be mixed out into the outer envelope of the star, saving it from being destroyed in the hydrogen burning shell. This explains why we see a jump in the surface lithium at this point in the star's lifetime. From here, there is no overlap between the convective region and the nuclear burning region which is why the surface lithium abundance remains essentially constant from this point, as the lithium just remains in this outer convective envelope.

4.4 Changing Mass

Several models of different masses were created and plotted onto the same graph shown in Figure 7 in order to compare their surface lithium levels. From this graph, it can be seen that this lithium production is definitely mass dependent. This is because the internal structure of a star is also mass dependent. The optimal mass for this lithium production lies around $82M_{\odot}$ and it can be seen that this model reaches the highest surface lithium abundance.

The distribution of maximum surface lithium with mass does not appear to be simple as it doesn't seem to always decrease the further the mass is away from its maximum value at $82M_{\odot}$— for example

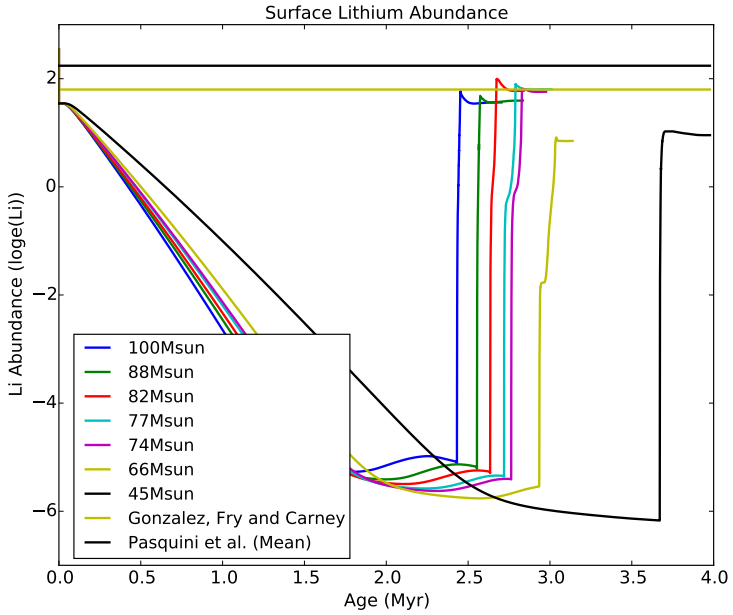

Figure 7: Plot of surface lithium for different masses with v=100km/s.

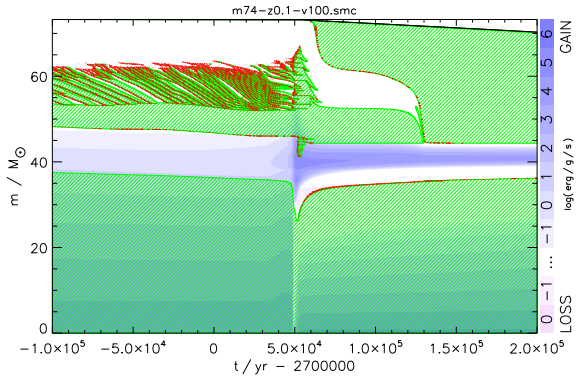

Figure 8: Kippenhahn Diagram for $74M_{\odot}$ model throughout its lifetime zoomed in at the time of lithium production.

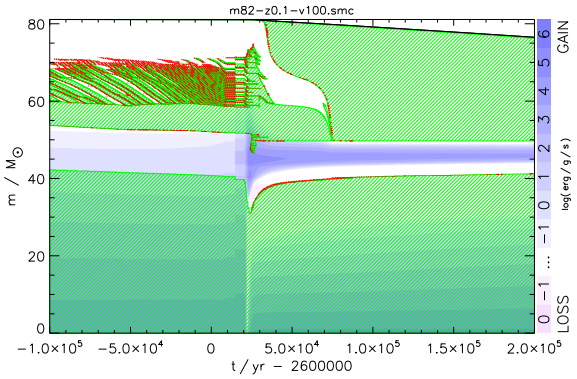

Figure 9: Kippenhahn Diagram for $82M_{\odot}$ model throughout its lifetime zoomed in at the time of lithium production.

the $100M_{\odot}$ model reaches a higher lithium abundance than the $88M_{\odot}$ model. A possible reason for the varying lithium production with mass is that the internal structure is slightly different for each model. The amount of time that stars have their convective region overlapping with their hydrogen burning shell could be a factor in explaining this variation in lithium production. This is shown on the Kippenhahn diagrams by the width of the overlapping region between the green convective region and the blue nuclear burning. The Kippenhahn diagrams produced for these models seem to agree with this idea— models that mix these regions for longer have a greater peak lithium value. Two of these Kippenhahn diagrams are shown in Figures 9 and 8 (zoomed in at the time of lithium production) and it can be seen that the model with higher lithium abundance (the $82M_{\odot}$ model) mixes for longer. Two more models' Kippenhahn diagrams are shown in Section A.1 for comparison.

4.5 Changing Rotational Velocity

Next, the initial rotational velocity of our models was changed to see how rotation affects this lithium production method in massive stars. Previously, the models considered have varied in mass but have had a constant initial rotational velocity of 100km/s. Figure 10 is a plot of how the surface abundance of lithium varies throughout time for each the models. The masses of these models were kept constant at $77M_{\odot}$ for this plot so the effect of rotational velocity could be investigated. The initial velocities are set at 50km/s, 75km/s, 100km/s and 125km/s.

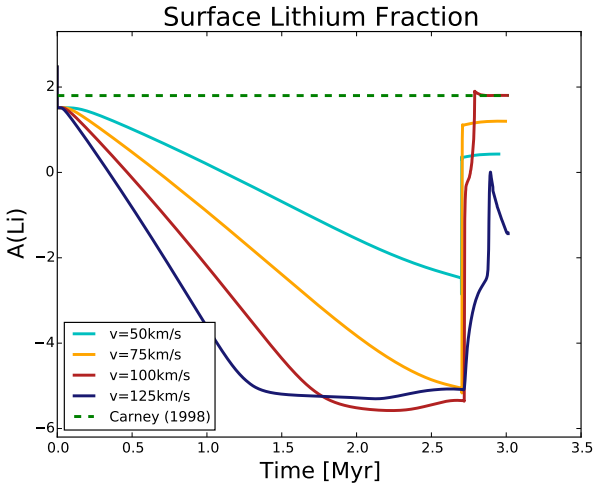

Figure 10: Plot of surface lithium for $77M_{\odot}$ models with v=50km/s, v=75km/s, v=100km/s and v=125km/s.

It can be seen that the initial rotational velocity has an effect on this lithium production method as the jump in surface lithium seems to be dependent on this value. The model with the highest surface lithium abundance once this production has taken place is the 100km/s model considered previously. We see the expected result where the models with lower rotational velocity deplete their surface lithium at a slower rate. This is because these stars have less rotational mixing and therefore the lithium-depleted material in the core is mixed out to the surface layers more slowly. If the rotation is increased too much, we see the lithium production is reduced, as shown by the 125km/s model. This is because increasing rotation means that more helium is transported out to the outer layers of the star by rotational mixing. This will increase the opacity of the star and therefore increase its temperature (Szécsi et al., 2015). This is shown in the models as the higher rotation models show a higher surface helium abundance (see Section A.2) which supports this interpretation. This higher rotation model becomes a blue supergiant due to this increase in temperature which causes a reduction of the convective envelope as shown in Section A.2. So, although there is still lithium production as the lithium is saved from the nuclear burning region, it is less in this model due to the smaller convective region.

Star's of a much higher rotational velocity have not been considered as candidates for pollution of lithium-enriched material as models have shown that increasing the rotational mixing of low metallicity, massive stars above $\sim$ 300km/s can cause the stars to become chemically homogeneous (Szécsi et al., 2015). This means that these fast rotating stars are not of interest when considering lithium production as the lithium will not remain in the star's envelope (which, in the case of chemically homogeneous models, is not convective) and will therefore be depleted.

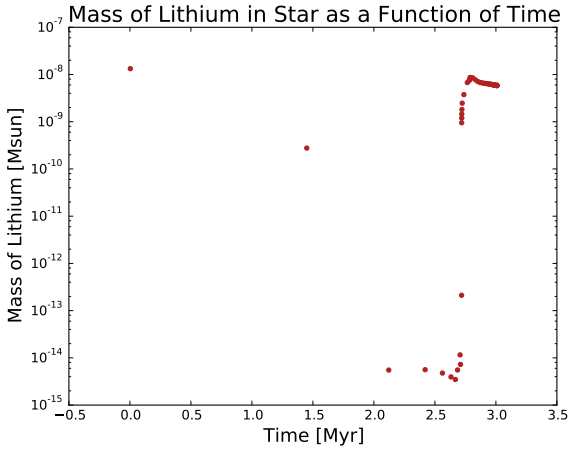

Figure 11: Plot of total lithium mass for $77M_{\odot}$ model throughout its lifetime.

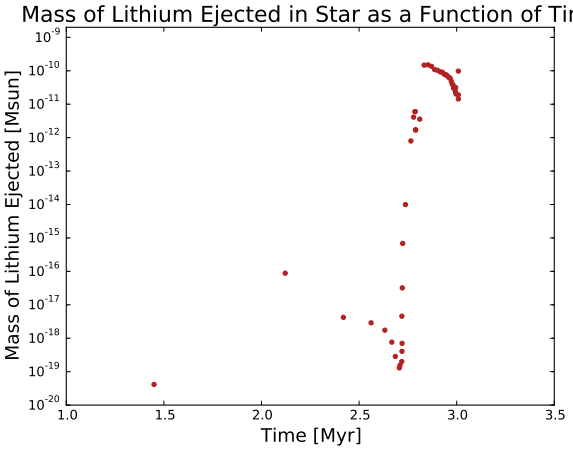

Figure 12: Plot of lithium mass ejected in stellar winds for $77M_{\odot}$ model throughout its lifetime.

4.6 Lithium Pollution

Next, the method of pollution of the intra-cluster medium must be considered so that this lithium-enriched material can form the next generation of stars. The simplest way of ejecting lithium from massive stars is by mass loss via stellar winds. For each model, the mass loss of the star was computed at every time step. This mass loss corresponds to losing a certain number of mass shells at the surface of the star due to stellar winds. Hence by considering the number of shells lost per time step and the relative abundance of lithium in each of these shells, a value of the lithium mass lost due to stellar winds can be calculated. This lithium mass loss has been plotted as a function of time as shown in Figure 12. The mass loss is largest (by several orders of magnitude) during the post-main sequence phase. This is when the star has started helium core burning and has expanded to thousands of times its initial radius. Because of this, the escape velocity at the surface of the star is much less than previously, meaning more mass is lost in stellar winds. This also corresponds to the time where the surface lithium abundance of the star jumps up (as in Figure 4) which means that this ejected material is very lithium rich. When considering mass loss by stellar winds, a cumulative value was taken over the star's entire lifetime as mass is gradually lost to the ICM.

Another possible mechanism of pollution is rapid stripping of the star's envelope by a binary companion star. To avoid detailed modelling of the mechanisms of binary stripping, we have computed the total mass of lithium throughout the star to obtain an upper limit for the amount of lithium that could pollute the intra-cluster medium. However, if we consider a case where the entire envelope of the star is stripped by a binary companion (where essentially all of the lithium lies) this total mass is not an unreasonable estimate. This was computed by integrating through all the mass shells of the model with their lithium fraction. Figure 11 shows how this total mass changes throughout the star's lifetime. When considering pollution, the maximum lithium mass in the star during its lifetime is taken as we assume a rapid stripping by a binary companion which will happen in a short amount of time relative to the star's lifetime. In order for maximum pollution, we assume that this stripping occurs at the point where the star has the highest amount of lithium.

Next, the amount of lithium pollution from an entire population of stars (for example in a globular cluster) was considered. To obtain an estimate for this value, the distribution of masses must be

considered— as given by the Salpeter initial mass function in equation (13). Using the initial mass function, the number of massive stars we would expect to find in each mass interval (for example in the range 74M$_\odot$ to 77M$_\odot$) can be calculated for a 10^6 star cluster as shown in equation (14). When considering these cluster values, it has been assumed that only stars in the mass range $45M_\odot$-$100M_\odot$ produce lithium. For masses that have not been modelled, the mean value of it's 2 nearest models was taken.

Table 2: Table showing the highest amount of lithium in each model and the total mass of lithium ejected in stellar winds throughout its lifetime. The last row shows these values scaled up for a 10^6 star cluster.

	Total Lithium Mass at Maximum [$M_\odot$]	Lithium Mass Ejected in Winds [$M_\odot$]
$45M_\odot$	7.12×10^{-10}	7.27×10^{-11}
$66M_\odot$	6.67×10^{-10}	6.81×10^{-11}
$74M_\odot$	5.62×10^{-9}	8.32×10^{-10}
$77M_\odot$	5.84×10^{-9}	1.46×10^{-9}
$82M_\odot$	6.11×10^{-9}	1.36×10^{-9}
$88M_\odot$	3.75×10^{-9}	1.42×10^{-9}
$100M_\odot$	3.42×10^{-9}	1.66×10^{-9}
10^6 star cluster	2.66×10^{-6}	4.53×10^{-7}

From these values, we can obtain a rough estimate for the number of high lithium stars that could be formed from this polluted material. This estimate assumes all the stars produced are solar mass stars with a lithium abundance of A(Li)=+2 (which is approximately where most of the observations lie for these abundance anomaly stars). However, this is still useful to get an order of magnitude estimate of how many stars this pollution scenario corresponds to.

$$\begin{aligned} A(Li) = \log_{10}\left(\frac{Li}{Li_\odot}\right) - \log_{10}\left(\frac{H}{H_\odot}\right) &= 2 \\ \log_{10}\left(\frac{Li}{H_\odot}\right) + 12 &= 2 \\ \log_{10}(Li) &= -10 \\ Li &= 10^{-10} \end{aligned} \tag{15}$$

So for $\sim 10^{-7}M_\odot$ of pollution of lithium enriched material in the cluster from stellar winds, this corresponds to an order of magnitude of approximately 10^3 stars being formed with a lithium abundance of A(Li)=+2. Similarly, for the case of binary stripping, this corresponds to an order of magnitude of approximately 10^4 stars being formed.

5 Conclusion

In conclusion, we have identified and described a new method of lithium production in massive stars which could in part explain observations of anomalous, high lithium stars in globular clusters. This lithium production takes place in the post-main sequence lifetime of a massive star when it is burning helium in its core. Lithium is produced as a by-product of the pp chain in stars but, in most cases, this lithium cannot escape the high temperatures of these nuclear burning regions before it is destroyed. However, in the case of these massive stars, lithium is produced in a hydrogen burning shell outside

of the helium burning core and their deep convective envelopes reach all the way from the surface to this region, meaning the lithium can be mixed out into the envelope where the temperatures are lower, saving it from being destroyed. This causes a sharp jump in the surface lithium abundance as the lithium is mixed into the stellar envelope, to a value which (depending on input parameters) is comparable to observations of high lithium abundance. While previously, enrichment scenarios did not explain both the anti-correlations of elements observed in globular clusters and the high lithium abundance, the models produced in this project have shown that these massive stars can pollute the ICM with material that has both high lithium abundance and characteristic anti-correlations.

The most lithium production takes place at a mass of $82M_{\odot}$ and at an initial rotational velocity of approximately 100km/s. The cause of the mass dependency of the lithium production is not immediately clear and it is likely that a lot of factors affect this. A possible reason is that different masses have a different amount of time where their outer convective envelope and hydrogen burning shell mix. For example, the $82M_{\odot}$ appears to have an overlap in these regions for longer than any other model, causing more lithium to be mixed into the envelope and therefore causing the high lithium abundance. While this appears to be consistent for the Kippenhahn diagrams we produced for these models, more intermediate mass models should be produced in order to check this interpretation.

For each model the maximum mass of lithium in the star throughout its lifetime and the total lithium mass ejected in stellar winds was computed. These values indicate how much lithium pollution can occur from these massive stars by binary stripping and stellar winds respectively. Using a Salpeter initial mass function, an order of magnitude estimate was obtained for the amount of lithium in stars and the amount of lithium in stellar winds in a star cluster from these massive stars. From this, we estimate up to 10^3 solar-mass stars could be produced from this lithium enriched material ejected in stellar winds by these massive stars in a cluster of 10^6 stars. By considering the total mass of lithium in this cluster, up to 10^4 stars could be formed from this polluted material although this assumes all this material can get into the ICM.

The mass range of $45M_{\odot}$-$100M_{\odot}$ has been considered in this project. When making estimates for the amount of pollution in a cluster, it was assumed that stars outside this range of masses do not produce lithium. More models of a wider range of masses should be made in order to check this assumption and to gain a more accurate value for the pollution in a cluster. Similarly, more intermediate mass models should be created inside this range as well as currently we assume, for example, an $80M_{\odot}$ star (which was not run) to have values averaged from the existing $77M_{\odot}$ and $82M_{\odot}$ models. Additionally, it would be more accurate to weight this average towards the lower mass model as, according to the initial mass function, lower mass stars are more abundant so more stars would lie below this simple average than above.

For future work, it would be useful to investigate the possibility of mass loss to the intra-cluster medium by binary stripping in more detail. These calculations for pollution by binary stripped set an upper limit and assume these stars are stripped at the optimal point in their lifetimes where the lithium mass in their envelopes is highest. This is because we assume that the most pollution is when the entire mass of lithium in the star (which is in the envelope) is stripped. In reality, not all of this material is always going to be stripped off by a binary companion star and of course many of these massive stars will not be in binary systems— nor in binary systems that will strip the star at optimal time. The maximum lithium mass in these stars corresponds to a time when they have already expanded greatly to close to their maximum radius (see plot in Section A.3). This does require more fine tuning of a binary system to ensure that the star will be stripped of its envelope at this time and no earlier.

Therefore, this value of pollution by a binary companion should be weighted by not only how many of these massive stars we expect to be in binary systems, but also how many of these binary systems will strip the star at such a time where it will contribute a significant amount of lithium to be polluted.

It would be also useful to factor the range of rotational velocities into the calculations shown in Table 2. In the same way the initial mass function was used to weight the different masses of models we used by how frequently they occur, a similar distribution should be used to give an idea of how many stars with a rotational velocity of 75km/s, for example, you would expect to find in a typical cluster. A possible distribution that could be used is given in Mokiem et al. (2006) which describes a Gaussian distribution with a mean of 160-190km/s and a half width of 100-150km/s. This is based on O type and B type stars (our models are O type stars when they are born) in the Small Magellanic cloud. Our models have a lower metallicity than this ($0.1Z_{smc}$) but there is not enough observational data of low metallity stars to form such a distribution. This would make the estimate of the cluster values more accurate as all the models used in this estimate had a rotational velocity of 100km/s. As seen in Figure 10, this is the optimal rotational velocity for lithium production out of all those modelled and therefore these cluster values provide an upper limit as not all these massive star would produce as much lithium.

Another alternative mechanism for forming the next generation of stars out of enriched material is suggested in Szécsi et al. (2017). This proposes a shell of star formation around a massive supergiant star in a globular cluster where the cold material ejected by stellar winds of the massive supergiant star meets an ionization front from external radiation. This causes up to 35% of the mass lost due to stellar winds from the massive supergiant star to be confined in an essentially static shell where star formation can take place. This applies to extremely massive stars which will exclude some of the lower mass stars we have modelled as candidates for this form of pollution. However, this mechanism is thought to occur down to stellar masses of $80M_{\odot}$ so stars in the mass range $80M_{\odot} - 100M_{\odot}$ could be candidates for both lithium production and this mechanism of enrichment. When considering pollution by other mechanisms, this enriched material is likely to become mixed with unprocessed gas in the ICM, diluting this enrichment. However, in this scenario explained above, the stars are formed entirely out of this processed material from the massive supergiant star and therefore would show this enrichment in their chemical make up.

References

L Bedin *Omega Centauri: the population puzzle goes deeper* , 2004

A Bellini *New Hubble space telescope WFC3/UVIS observations augment the stellar-population complexity of ÏĽ Centauri* , 2010

B. Carney *Lithium and r-Process Abundances in the Population II Cepheid M5 V42* , 1998

G Chabrier *Galactic Stellar and Substellar Initial Mass Function* ,2003

C. De Loore *Evolution of massive stars with mass loss by stellar wind* , 2012

P A Denissenkov *The puzzling MgAl anticorrelation in globular-cluster red giants: primordial plus deep mixing scenario?* , 1997

P A Denissenkov *The primordial and evolutionary abundance variations in globular-cluster stars: a problem with two unknowns* , 2015

B D Fields *Big Bang Nucleosythesis* , 2013

R Gratton *Abundance Variations in Globular Clusters* , 2004

W Harris *Globular Cluster Systems in Brightest Cluster Galaxies: Bimodal Metallicity Distributions and the Nature of the High-Luminosity Clusters* , 2006

V Henault-Brunet *Multiple populations in globular clusters: the distinct kinematic imprints of different formation scenarios* , 2015

H Janka *Theory of core-collapse supernovae* , 2006

Y Li *Red supergiant variables in the Large Magellanic Cloud: Their evolution and pulsations* , 1994

A Liddle *An Introduction to Modern Cosmology* , 2013

M Mokiem *The VLT-FLAMES survey of massive stars: mass loss and rotation of early-type stars in the SMC* , 2006

L. Monaco *Lithium and sodium in the globular cluster M4: Detection of a Li-rich dwarf star: preservation or pollution?* , 2012

L. Pasquini *Li in NGC 6752 and the formation of globular clusters* , 2005

A. Pilachowski *A Survey for Enhanced Lithium in 261 Globular Cluster Giants* , 2000

N. Prantzos *Light nuclei in galactic globular clusters: constraints on the self-enrichment scenario from nucleosynthesis* , 2007

E Salpeter *The luminosity function and stellar evolution* , 1955

D Szécsi *Low-metallicity massive single stars with rotation* , 2015

D Szécsi *Supergiants and their shells in young globular clusters* , 2017

P Ventura *A deep insight into the MgâĂŞAlâĂŞSi nucleosynthesis in massive asymptotic giant branch and super-asymptotic giant branch stars* , 2011

S Yoon *Evolution of massive stars with pulsation-driven super-winds during the red supergiant phase* , 2013

A Appendix

A.1 Kippenhahn Diagrams

More Kippenhahn diagrams are presented in order for comparison of the time where the convective and nuclear burning regions overlap, as this seems to correlate to the amount of lithium produced. These are zoomed in at this time to see the overlap more clearly.

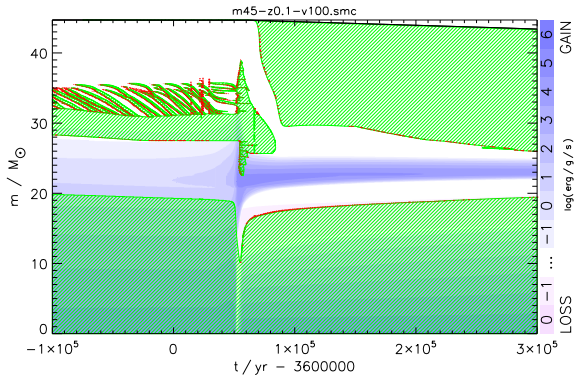

Figure 13: Kippenhahn diagram for $45M_{\odot}$ model throughout its lifetime zoomed in at the time of lithium production.

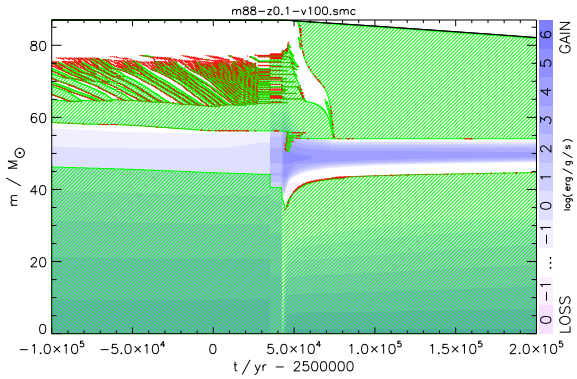

Figure 14: Kippenhahn diagram for $88M_{\odot}$ model throughout its lifetime zoomed in at the time of lithium production.

A.2 High Rotation Model

The central and surface helium fraction of 2 models are plotted in Figure 15 and 16 to show that higher rotation models mix out more helium to the surface, which will increase the opacity and temperature of the star and therefore reduce the convective regions. A Kippenhahn diagram for the 125km/s model is shown in Figure 17 which shows the reduction of the convective region for this model due to its high temperatures. Other models have a convective envelope that reaches all the way to the surface at the start of the star's helium core burning lifetime, but in this model, it doesn't reach the surface. This is the reason for the reduced lithium production.

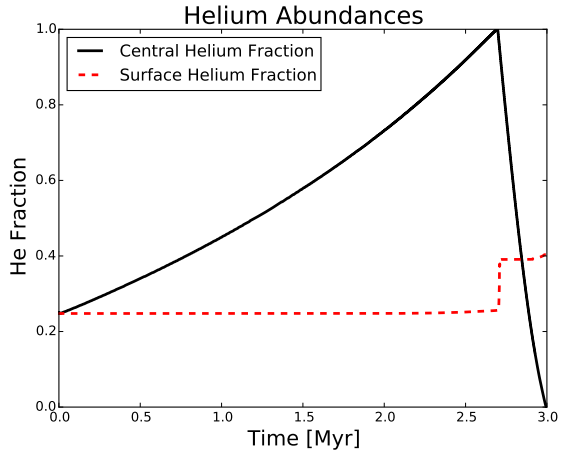

Figure 15: Plot of surface and core helium abundance for $77M_{\odot}$, v=75km/s model throughout its lifetime.

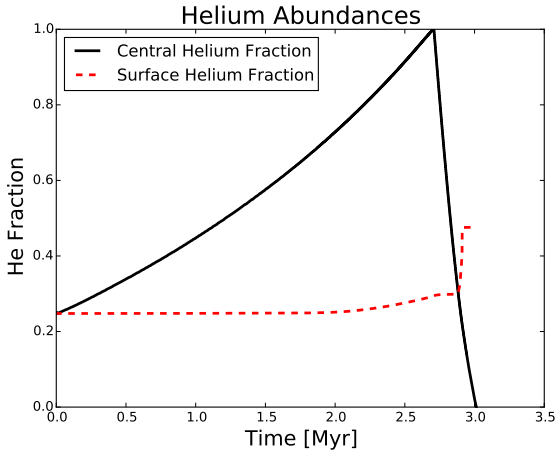

Figure 16: Plot of surface and core helium abundance for $77M_{\odot}$, v=125km/s model throughout its lifetime.

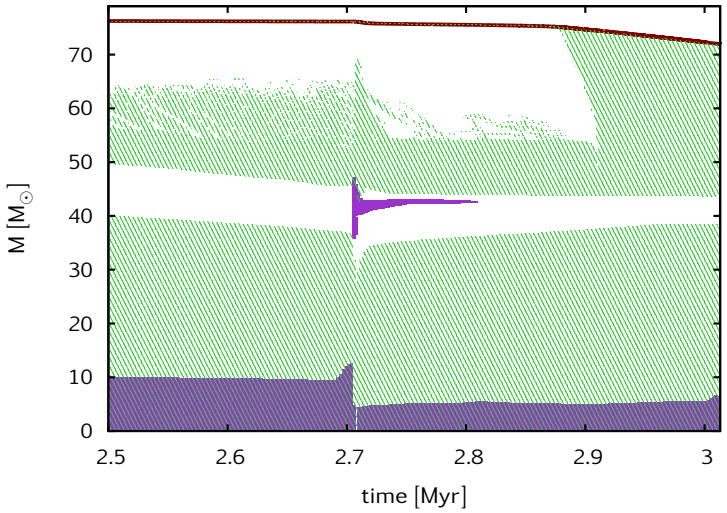

Figure 17: Kippenhahn Diagram for $77M_{\odot}$, 125km/s model throughout its lifetime zoomed in at the time of lithium production, showing the reduced convective region due to high temperatures.

A.3 Radius Plot

The surface lithium abundance and the radius of the star have been plotted on the same graph for the $77M_{\odot}$ model in Figure 18. It can be seen that the maximum lithium abundance occurs once the star has already greatly expanded in radii which puts limits on the amount of binary systems that can strip the star at this point.

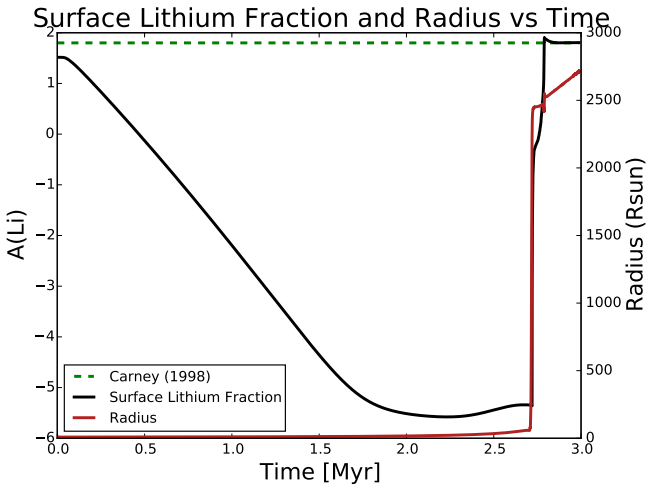

Figure 18: Plot of surface lithium and radius against time for $77 M_{\odot}$ model.